

Quantum-chemical, NMR and X-ray diffraction studies on (\pm) -1-[3,4-(methylenedioxy)phenyl]-2-methylaminopropane

Gerald Zapata-Torres^{a,*}, Bruce K. Cassels^b, Julia Parra-Mouchet^b,
Yvonne P. Mascarenhas^c, Javier Ellena^c, A.S. De Araujo^c

^aDepartamento de Química Inorgánica y Analítica, Facultad de Ciencias Químicas y Farmacéuticas,
Universidad de Chile, Olivos 1007, Independencia, Santiago, Chile

^bDepartamento de Química, Facultad de Ciencias, Universidad de Chile, Casilla 653, Santiago, Chile

^cInstituto de Física de São Carlos, Universidade de São Paulo, C.P. 369, 13560-970 São Carlos, SP, Brazil

Received 30 August 2007; received in revised form 18 December 2007; accepted 19 December 2007

Available online 4 January 2008

Abstract

Time-averaged conformations of (\pm) -1-[3,4-(methylenedioxy)phenyl]-2-methylaminopropane hydrochloride (MDMA, “ecstasy”) in D₂O, and of its free base and trifluoroacetate in CDCl₃, were deduced from their ¹H NMR spectra and used to calculate their conformer distribution. Their rotational potential energy surface (PES) was calculated at the RHF/6-31G(d,p), B3LYP/6-31G(d,p), B3LYP/cc-pVDZ and AM1 levels. Solvent effects were evaluated using the polarizable continuum model. The NMR and theoretical studies showed that, in the free base, the *N*-methyl group and the ring are preferentially *trans*. This preference is stronger in the salts and corresponds to the X-ray structure of the hydrochloride. However, the energy barriers separating these forms are very low. The X-ray diffraction crystal structures of the anhydrous salt and its monohydrate differed mainly in the *trans* or *cis* relationship of the *N*-methyl group to the α -methyl, although these two forms interconvert freely in solution. © 2007 Elsevier Inc. All rights reserved.

Keywords: MDMA; nAChR; NMR; Semi-empirical and *ab initio* calculations; X-ray structure

1. Introduction

(\pm) -1-[3,4-(Methylenedioxy)phenyl]-2-methylaminopropane (methylenedioxymethamphetamine, “MDMA”, Fig. 1) [1], is the prototype of a small series of psychoactive substances commonly termed “entactogens” [2]. “This compound widely used as a recreational drug” [3,4] has been reported as a relatively selective dopaminergic neurotoxin in mice [5]. Nicotine produces effects comparable to those of MDMA on dopamine release [6]. As a consequence, it has been the subject of a large number of scientific publications on its pharmacology and toxicology where adverse MDMA effects are usually ascribed to neurotransmitter release in the central nervous system. Although there is no agreement regarding the mechanism(s) underlying the subjective effects of MDMA, its monoamine-releasing actions seem to play a dominant role

[7], with some contribution from its direct effects on serotonin receptors [8]. Previous studies have demonstrated the participation of α -7 nicotinic receptors (nAChR) in the neurotoxic effect of methamphetamine. In vivo, methyllycconitine (MLA), a specific α -7 nAChR antagonist, significantly prevented MDMA-induced neurotoxicity at the dopaminergic but not serotonergic level [5]. MDMA induces Ca²⁺ transients in myotubes and increases their acidification rate. However another specific antagonist of nAChR, α -bungarotoxin, abolished these MDMA effects. The nAChR agonistic action of MDMA has been confirmed by patch-clamp measurements of ion currents on human embryonic kidney cells expressing nAChR [9].

In 1985, a World Health Organization (WHO) Expert Committee on Drug Dependence recommended placing MDMA on Schedule I (meaning that it has no medical use and a high potential for abuse), and its possession, distribution and manufacture were promptly declared criminal offences, initially in the USA and subsequently in many other countries. Nevertheless, in the last few years several clinical studies have

* Corresponding author. Tel.: +56 29782961.

E-mail address: gzapata@uchile.cl (G. Zapata-Torres).

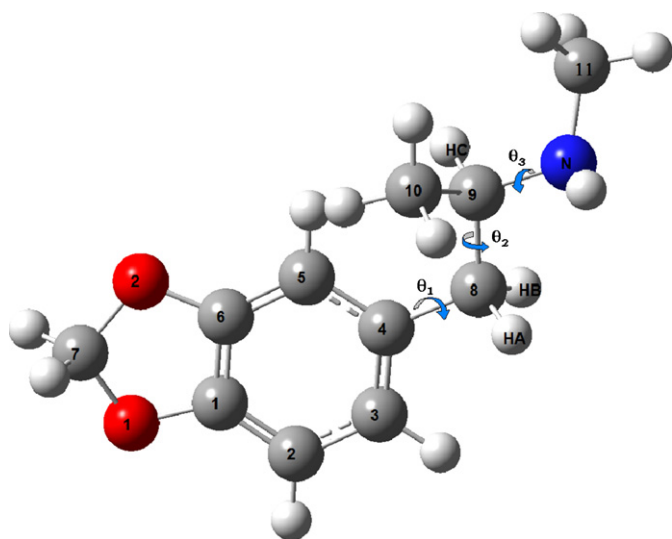


Fig. 1. Structural formula of (±)-1-[3,4-(methylenedioxyphenyl)]-2-methylaminopropane. Numbering is according to the crystal structure of Morimoto et al. [11]. The curved arrows indicate the torsion angles θ_{1-3} .

begun to explore the use of MDMA in the treatment of post-traumatic stress disorder [10].

The conformational mobility of a flexible drug molecule plays an important role in its interaction with its biological binding site(s) and presumably has a profound influence on its pharmacological properties. To investigate the conformational space of MDMA as the free and protonated base in D_2O and in $CDCl_3$ at a molecular level, we carried out NMR studies using 1H NMR coupling constants. Since spin-lattice relaxation times (T_1) as well as chemical shifts change with concentration, solvent and temperature, these parameters were not included to study conformational preferences, thus avoiding erroneous conclusions.

Quantum-chemical calculations (*ab initio* and semiempirical) including solvent effects were performed to shed light on the energetics of the intramolecular rotations. Finally, we compared the published X-ray structure of anhydrous MDMA hydrochloride [11] with the crystallographic structure of a monohydrate obtained in our laboratories.

2. Materials and methods

2.1. Chemistry

(±)-MDMA was synthesized by reductive amination of piperonylmethylketone as described in the literature [1]. 1H and ^{13}C NMR spectra were recorded for MDMA free base and its trifluoroacetate in $CDCl_3$, and for its hydrochloride in D_2O , at 300 MHz (1H) and 75 MHz (^{13}C) using a Bruker AMX-300 spectrometer. ^{13}C spin-lattice relaxation times were determined on deoxygenated samples (prepared by bubbling N_2 in the sample tube), using 180° , τ , 90° (inversion-recovery) pulse sequences controlled by standard Bruker software. While recovering a sample of MDMA-HCl, a crop of colourless flat rhombic parallelepipeds was obtained which was obviously different from the more compact crystals of the anhydrous salt.

This material, in spite of its clean 1H NMR spectrum in D_2O , did not exhibit a sharp melting point under the microscope (Cambridge Instruments Reichert-Jung Galen III). With slow heating it began to melt at about $80^\circ C$, promptly crystallized again exhibiting sharp right angles, softened again from $88^\circ C$, melted almost completely at $135^\circ C$ with some new crystals forming on the edges of the melt, which disappeared at $140^\circ C$. One of the tabular crystals was selected for X-ray diffraction.

2.2. X-ray analysis

The measurements were made at room temperature on an Enraf-Nonius KAPPA CCD diffractometer (95 mm CCD camera on κ -goniostat) with graphite monochromated $Mo K\alpha$ ($\lambda = 0.71703 \text{ \AA}$) radiation. Data collection (φ scans and ω scans with κ offsets) used the COLLECT Program; [12] integration and scaling of the reflections was performed with the HKL DENZO SCALEPACK set of programs [13]. Data were collected up to 50° in 2θ , with a redundancy of 4. The final unit cell parameters were based on all reflections using HKL-SCALEPACK [13]. The structure was solved using the direct method and refined by the full-matrix least squares procedure on F^2 with SHELXS-97 [14]. Hydrogen atoms were set to be isotropic and freely refined. The WINGX [15] program was used to analyze and prepare the data for publication. Crystal data, data collection procedures, structure determination methods and refinement results are summarized in Table 1. The ORTEP representation was prepared using ORTEP-3 for Windows (Fig. 2) [15]. Atomic and thermal vibration parameters and other crystallographic structural data have been deposited with the Cambridge Crystallographic Data Centre as CCDC 292512.

2.3. Quantum-chemical studies

2.3.1. Equilibrium structures of MDMA

The MDMA molecule in its neutral and protonated forms possesses a fundamental framework containing three torsional degrees of freedom. These involve the twist angles θ_1 , [C5–C4–C8–C9 sequence], θ_2 [C4–C8–C9–N sequence], and θ_3 , [C8–C9–N–C11 sequence], illustrated in Fig. 1. Rotation around θ_2 generates three rotamers depicted in Fig. 3: the “extended” or *anti* one (A) has $\theta_1 = 90^\circ$, $\theta_2 = -180^\circ$, with the benzene ring and the *N*-CH₃ group in an *anti* relationship around the C8–C9 bond; and two “folded”, *gauche* or *syn* ones (*S*₁ and *S*₂, respectively) having $\theta_1 = 90^\circ$, $\theta_2 = -60^\circ$ and $\theta_1 = 90^\circ$, $\theta_2 = 60^\circ$, respectively, with the ring and the *N*-CH₃ group in a *syn* relationship around the same bond.

Full geometry optimizations were carried out in vacuo using both the semi-empirical AM1 method and the RHF/6-31G(d,p) level of theory. For the DFT calculations, Becke’s three-parameter hybrid functional (B3) together with the correlation functional of Lee, Yang and Parr (LYP) and Dunning’s cc-pVDZ basis set were employed as implemented in the Gaussian 98 package of programs [16]. Solvent effects on the conformational and electronic structure of MDMA and its *N*-protonated conjugate acid, with the dielectric constant fixed

Table 1

¹H chemical shifts and vicinal coupling constants of side-chain protons^a, and conformer distribution^b in free base and protonated MDMA

Compound	Solvent	Chemical shifts (ppm) ^a			Vicinal coupling constants (Hz) ^{a,b}			Conformer distribution ^b		
		<i>H</i> _A	<i>H</i> _B	<i>H</i> _C	<i>J</i> _{AC}	<i>J</i> _{BC}	<i>J</i> _{AB}	A	<i>S</i> ₁	<i>S</i> ₂
Free base	CDCl ₃	2.59	2.54	2.73	6.9	6.4	13.4	0.44 ^c	0.37 ^c	0.19 ^c
Hydrochloride	D ₂ O	2.81	2.97	3.47	7.8	6.4	14.0	0.58 ^d	0.42 ^d	0.00 ^d
Trifluoroacetate	CDCl ₃	2.66	3.15	3.26	10.3	4.2	13.3	0.82 ^e	0.18 ^e	0.00 ^e

^a ¹H NMR spectra were recorded at 300 MHz using 0.1 M solutions, δ relative to TMS (CDCl₃) or TMSPA-*d*₄ sodium salt (D₂O); *T* = 300 K.^b Calculated from experimental spectra.^c Calculated assuming *J*_g = 2.8 Hz and *J*_t = 12.3 Hz.^d Calculated assuming *J*_g = 2.6 Hz and *J*_t = 11.7 Hz.^e Calculated assuming *J*_g = 2.4 Hz and *J*_t = 11.9 Hz.

at $\varepsilon = 78.3$, were introduced by means of SCRF methods based on PCM [17]. The relaxed potential energy surface (PES) scans of MDMA were carried out at 10° intervals along the torsional angles θ_1 and θ_2 . θ_3 was not scanned because the NMR results showed free rotation around this torsional angle. The θ_1 and θ_2 values were increased for anticlockwise rotation from the standard position as in Fig. 1 ($\theta_1 = 0^\circ$, $\theta_2 = -180^\circ$, respectively). The runs were also carried out on protonated MDMA and in the presence of its counterions chloride and trifluoroacetate.

3. Results and discussion

3.1. NMR conformational analysis

In order to explore the time-averaged conformer distribution of MDMA, we used the vicinal proton coupling constants (³*J*) determined from the ¹H NMR spectra. The coupling constants were correlated with the θ_2 torsion angle around the central C8–C9 bond, based on the Karplus equation [18], where the relative

populations of these rotamers are given by *a*, *b* and *c*, respectively: [19]

$$a = \frac{[J_{AC} - J_g]}{[J_t - J_g]}$$

$$b = \frac{[J_{BC} - J_B]}{[J_t - J_g]}$$

$$c = \frac{[(J_t + J_g) - (J_{AC} - J_{BC})]}{[(J_t - J_g)]}$$

All calculations included *J*_g and *J*_t terms for the coupling constants of perfectly *gauche* and *trans* vicinal protons [20] where *J*_{AC} and *J*_{BC} correspond to the coupling constants between *H*_A, *H*_C and *H*_B, *H*_C protons, respectively (see Fig. 3). These ³*J* values represent time-averaged conformations and may be regarded as the weighted means of the mixtures of the most stable rotamers, approximated by the perfectly staggered conformations (A, *S*₁ and *S*₂; see Fig. 3) around the C8–C9 bond.

The populations of the three hypothetical completely staggered rotamers around the C8–C9 bond can be estimated from the apparent ³*J*^{HH} coupling constants of the side chain hydrogen nuclei if appropriate parameters are chosen to represent the coupling constants of perfectly *trans* and *gauche* protons (*J*_t and *J*_g, respectively). The uncertainties attached to this method have been discussed by Makriyannis and Knittel working with related compounds [21]. In early publications on amphetamine derivatives, *J*_t = 12.0 Hz and *J*_g = 2.0 Hz were

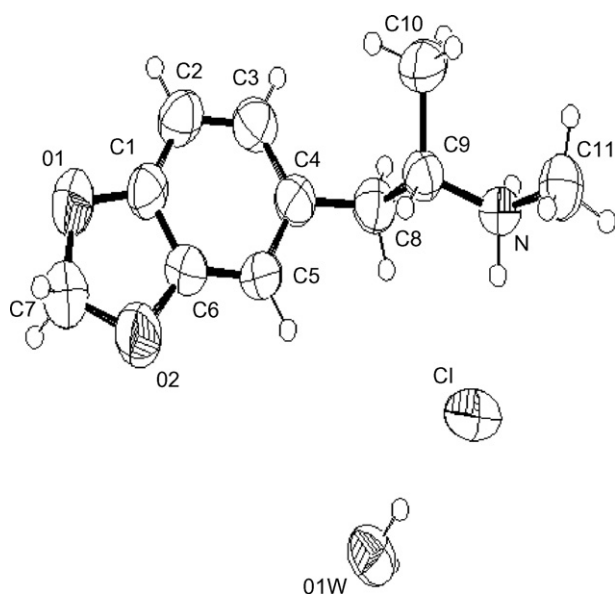


Fig. 2. ORTEP3 view of MDMA hydrochloride monohydrate showing the atom-labelling scheme. Displacement ellipsoids drawn at 50% probability. H atoms are represented by circles of arbitrary size.

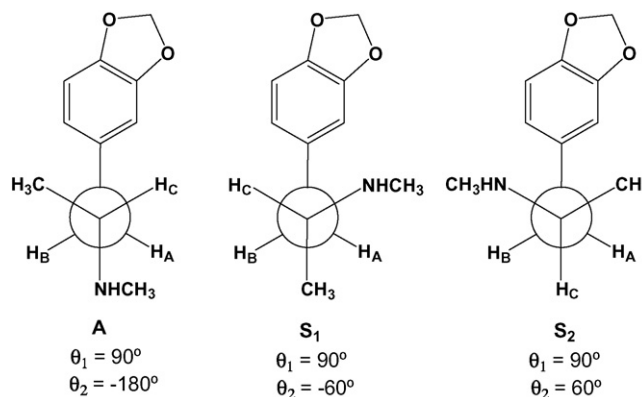


Fig. 3. The three idealized completely staggered rotamers of MDMA around the C8–C9 bond.

used for samples dissolved in CDCl_3 [19] and $J_t = 13.0$ Hz and $J_g = 2.0$ Hz were used for aqueous solutions [22]. Makriyannis and Knittel [21] preferred a combination of values calculated for a conformationally rigid model compound ($J_t = 11.0$ Hz and $J_g = 3.5$ Hz), using Abraham and Gatti's empirical relationship [23] between vicinal proton coupling constants and the electronegativities of substituents on C8 and C9 of ethane ($J_t = 13.11$ Hz and $J_g = 3.63$ Hz). In the latter case, the Huggins electronegativities [24] of carbon and nitrogen ($x_C = 2.60$ and $x_N = 3.05$), based on average bond energies, were used.

It is generally acknowledged that the electronegativity of carbon atoms varies in the sequence $sp > sp^2 > sp^3$, and values such as $x_{\text{methyl}} = 2.3$ and $x_{\text{phenyl}} = 3.0$ have been estimated [25]. Similarly, protonation of a nitrogen atom raises its electronegativity from $x_{\text{amino}} = 3.35$ to $x_{\text{ammonio}} = 3.8$. Recalculation of J_t and J_g for phenethylamine, using the above electronegativities for phenyl carbon and amino nitrogen, gives 12.48 and 2.97 Hz, respectively. Protonation of the amino group would be expected to alter these values to 12.09 and 2.55 Hz.

Furthermore, in amphetamine derivatives, the carbon atom bearing the amino (or ammonio) substituent carries a methyl group which might also affect J_t and J_g . As noted by Abraham and Gatti [23], vicinal proton coupling constants generally decrease with increasing electronegativity of the substituents. If a hydrogen atom on C8 or C9 is replaced by a methyl group, and the effect of a third substituent on the ethane moiety is assumed to be additive, the sum of the electronegativities may be expected to increase by about 0.2, with J_t and J_g decreasing by about 0.18 and 0.19 Hz, respectively. This line of reasoning leads to our choosing $J_t = 12.3$ Hz and $J_g = 2.8$ Hz for the free bases and $J_t = 11.9$ Hz and $J_g = 2.4$ Hz for the salts in a low-polarity medium like CDCl_3 . Finally, vicinal coupling constants vary with the dielectric constant ϵ of the medium, with J_t decreasing and J_g increasing slightly with increasing values of ϵ [23]. Thus, following these authors, more appropriate parameters for aqueous solutions of salts of amphetamine derivatives might be $J_t = 11.7$ Hz and $J_g = 2.6$ Hz. The relevant ^1H NMR data and the conformer distributions of MDMA free base and its salts in CDCl_3 and in D_2O , calculated using the J values proposed by us, are summarized in Table 1.

In CDCl_3 , the “extended” A rotamer of the free bases of *N*-unmethylated, ring-substituted amphetamine derivatives clearly predominates (mole fraction 0.62–0.67) [19], and the situation for the MDMA free base appears to be similar when using the same J_g and J_t values (0.49). Makriyannis and Knittel found mole fractions of 0.61 and 0.27 for the “extended” and “folded” forms of amphetamine free base in CDCl_3 [26]. These results are in fairly good agreement with our results for MDMA using their J terms (0.46 and 0.38, respectively). With the parameters calculated by us for free amines, we obtain mole fractions of 0.44 and 0.37 for rotamers A and S_1 , suggesting that the preference for the “extended” form might not be so great. The “folded” conformer S_2 presents both the amine nitrogen and the C10 methyl group in *gauche* arrangements with regard to the benzene ring, and is thus the least favored.

According to Neville et al. [22], in aqueous solution the “extended” conformation of amphetamine derivatives, with an *anti* relationship between the aromatic ring and the amino group is only slightly preferred (mole fractions 0.47–0.55) over the “folded” one with a *syn* relationship between these moieties (0.36–0.45). Benzphetamine hydrochloride is an exception, with a ratio of 0.64–0.35, presumably due to the large volume of the *N*-benzyl substituent. Using the Neville et al. values for J_t and J_g , our results for MDMA hydrochloride were intermediate between these values (0.53 for rotamer A vs. 0.40 for rotamer S_1), as expected for an *N*-methylated derivative. The parameters suggested by Makriyannis and Knittel ($J_t = 11.0$ Hz, $J_g = 3.5$ Hz) give mole fractions of 0.58 and 0.39 for the most favored rotamers [21,26] which differ significantly from the practically identical contributions found by these authors for both forms of *N*-unmethylated amphetamine hydrochloride and its 4-methoxy- and 3,4,5-trimethoxy derivatives in D_2O . Increasing both parameters to the values calculated by Makriyannis and Knittel [21], using Abraham and Gatti's equations [16,23] ($J_t = 13.11$ Hz, $J_g = 3.63$ Hz) leads to the prediction of practically equal populations (0.29 and 0.26) for the two less favored completely staggered rotamers, which is counterintuitive. With our choice of $J_t = 11.7$ Hz and $J_g = 2.6$ Hz, we have calculated mole fractions of 0.58 and 0.42 for the preferred rotamers (and 0 for the least favored one). Thus, in aqueous solution, protonated MDMA should exist mainly as the “extended” conformer A, although the contribution of the “folded” form S_1 is by no means negligible, while rotamer S_2 is practically absent, unlike the situation found for the free base in CDCl_3 where these less favored conformers may contribute significantly to the equilibrium mixture. An increased preference for the rotamer with a *trans* relationship between the benzene ring and the nitrogen atom seems reasonable, considering that in aqueous solution the ammonium function should be strongly hydrated, and that its effective volume should thus be much greater than that of the naked amino group in CDCl_3 [27].

Amine drug molecules are believed to interact with biological macromolecules as protonated ammonium ions, rather than as uncharged free bases. Also, low-polarity solvents presumably mimic the internal milieu of protein molecules better than water. Therefore, studies of salts of phenethylamine derivatives in solvents with low dielectric constants are probably much more relevant to their pharmacological activities than measurements carried out on free bases or on aqueous salt solutions. The first experimental studies considering these aspects seem to be those of Makriyannis and Knittel, who analyzed the ^1H NMR spectra of the hydrochlorides of amphetamine and 1-phenyl-2-butanamine analogues in CDCl_3 [21,26]. Their results were interpreted to indicate that “extended” rotamers predominate more strongly in this solvent than in D_2O , with typical mole fractions of 0.76–0.77 vs. 0.21–0.23 for the more stable “folded” conformer and 0.01–0.03 for the least stable one. Using these authors' values, we obtained good correlations. On the other hand, incorporating the corrections suggested by Abraham and Gatti [23], we arrived at the absurd prediction that the S_2 conformation is

preferred over the S_1 . With our calculated figures of $J_t = 11.9$ Hz and $J_g = 2.4$ Hz, we find that 82% of the molecules are in the “extended” conformation, as expected if protonated MDMA and its fairly large trifluoroacetate counterion form tight ion pairs in $CDCl_3$. The S_2 conformation is negligible.

In summary, the distribution of conformers obtained from the measured coupling constants for MDMA in its free base form, dissolved in $CDCl_3$, shows a slight preference for the “extended” rotamer A. In that conformation the phenyl group is *anti* to the methylamino group and *syn* to the methyl group bonded to the methine carbon. This conformer distribution shows a somewhat smaller population of S_1 and an even smaller S_2 population, in which both the $N-CH_3$ group and the α -methyl group are *gauche* with regard to the benzene ring. When MDMA trifluoroacetate is dissolved in $CDCl_3$, it seems to exist almost exclusively in the “extended” form A. In aqueous solution, protonated MDMA exists mainly as the “extended” conformer A, although the contribution from the “folded” or *syn* form S_1 is also quite considerable, while rotamer S_2 is practically absent, as found for the trifluoroacetate in $CDCl_3$. An increased preference for rotamer A with a *trans* relationship between the benzene ring and the nitrogen atom seems reasonable for the hydrochloride, considering that in aqueous solution the ammonium function should be strongly hydrated, and that its effective volume should thus be much greater than that of the naked amino group in $CDCl_3$ [27].

These results are in agreement with the published value for the torsion angle of the α -methyl group C10 and the phenyl ring of $-66.4(3)^\circ$ in the anhydrous MDMA hydrochloride crystal [11]. The introduction of an N -methyl substituent clearly affects the rotational energy profile of phenethylamines since it is known that compounds such as DOET (2,5-dimethoxy-4-ethylamphetamine), and TMA (2,4,5-trimethoxyamphetamine) have torsion angles of 178° [24] and 170° [25], respectively.

3.2. Quantum-chemical studies

3.2.1. Rotational barriers of MDMA

Potential energy profiles for the internal rotation of the θ_1 and θ_2 bonds of MDMA are shown in Figs. 4 and 5. 3D PES Scan and contour plot is shown in Fig. 6, and for its N -protonated form in Figs. 7 and 8, respectively.

3.2.2. C4–C8 bond

Rotation about the C4–C8 bond in the neutral molecule (optimizing the torsion angle θ_2 throughout this rotation, see Fig. 4) showed that the conformation with a dihedral angle θ_1 of approximately 70° represents a global minimum on the RHF/6-31G(d,p), B3LYP/6-31G(d,p), and B3LYP/cc-pVDZ rotational potential energy surfaces (PES). A second local minimum is 0.23 kcal mol $^{-1}$ (at RHF/6-31G(d,p) level), and 0.17 kcal mol $^{-1}$ higher in energy corresponding to a θ_1 value of 260° at the same levels of calculation (B3LYP/6-31G(d,p) and B3LYP/cc-pVDZ). This almost *trans* (antiperiplanar) relationship is in agreement with the NMR results and the monohydrated crystal structure.

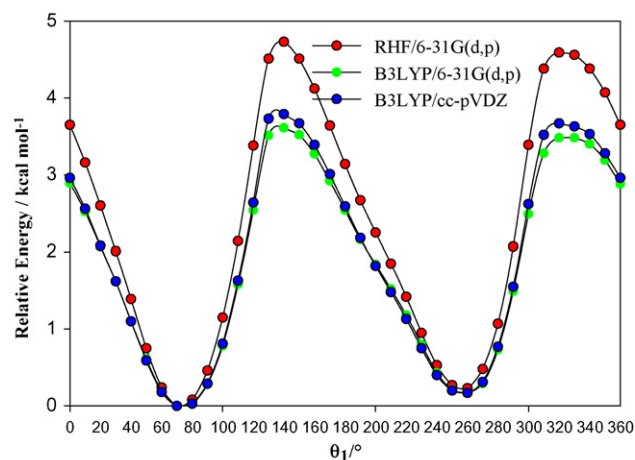


Fig. 4. Conformational energy of neutral MDMA as a function of rotation of θ_1 , optimizing θ_2 , at the RHF/6-31G(d,p), B3LYP/6-31G(d,p) and B3LYP/cc-pVDZ levels.

3.2.3. C8–C9 bond

Fig. 5 shows the relative rotational energy around θ_2 (for a fixed θ_1 value of 70° obtained from the relaxed PES scan described above at the same levels of calculation). The internal rotational energy profile determines the most stable rotamers in MDMA, according to Fig. 3. The curve shows three local minima, two of them corresponding to two “folded” conformations, with dihedral angles $\theta_2 \approx -60^\circ$ (resembling S_1) and $\theta_2 \approx -60^\circ$ (resembling S_2). With the exception of B3LYP/cc-pVDZ, we found an “extended” conformation (resembling form A) to be the global minimum and S_1 -like and S_2 -like conformers to be local minima on the rotational potential energy surface (PES). The energy difference between the minima and the height of the rotational barrier depends on the basis set used. The 6-31G(d,p) and cc-pVDZ basis sets give rather small relative energy differences between A and S_1 -like conformers (0, 0.05, 0.24 kcal mol $^{-1}$ with B3LYP/cc-pVDZ, B3LYP/6-31G(d,p) and RHF/6-31G(d,p), respectively) and S_2 -like conformers (0.16, 1.17, 1.87 kcal mol $^{-1}$ with B3LYP/cc-

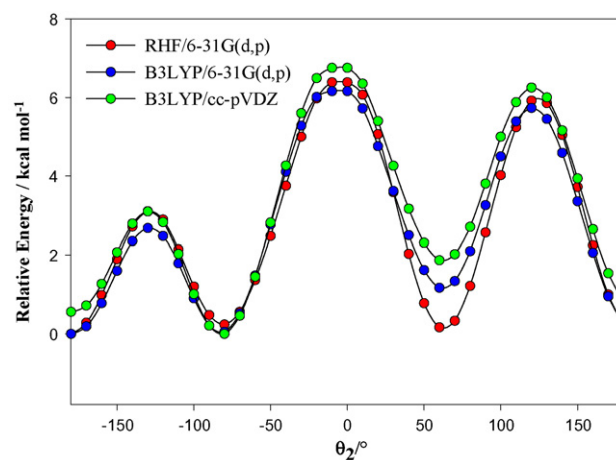


Fig. 5. Conformational energy of neutral MDMA as a function of θ_2 with θ_1 fixed at 70° (obtained from relaxed PES scan) at the RHF/6-31G(d,p), B3LYP/6-31G(d,p) and B3LYP/cc-pVDZ levels.

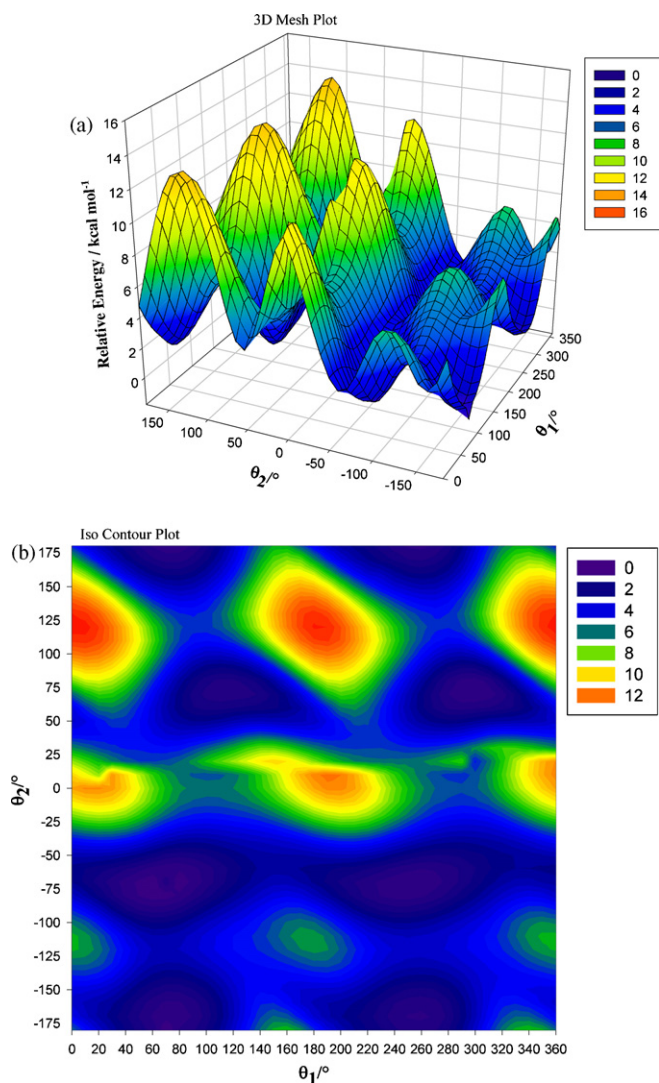


Fig. 6. The MDMA torsional potential energy surface (a) the 3D-mesh plot, (b) the iso-value contour plot for MDMA.

pVDZ, B3LYP/6-31G(d,p) and RHF/6-31G(d,p), respectively). The rotational PES found with AM1 shows the same trend but the three local minima are separated by very low rotational barriers (data not shown). The S_1 -like conformers should therefore be quite densely populated and in rapid equilibrium with each other. The internal rotational barrier of the S_2 -like conformer, on the contrary, suggests a much lower abundance than those of the other two conformers, in good agreement with the calculated conformer population.

3.2.4. Three-dimensional potential surfaces

The potential surface scan for the internal rotation of both the C5–C4–C8–C9 moiety and C4–C8–C9–N fragment denoted by θ_1 and θ_2 about the C–C single bonds was obtained by allowing the dihedral angle (θ_1) to increase in 10° steps from 0° to 360° at a constant N–C9–C8–C5 dihedral angle (θ_2). Full energy optimisations were repeated for each value of θ_2 every 10° from 0° to 360° at the B3LYP/6-31G(d,p) level. This gave rise to a total of 1369 data points that were enough to depict the 3D surface scan and contour plot as shown in Fig. 6. From this

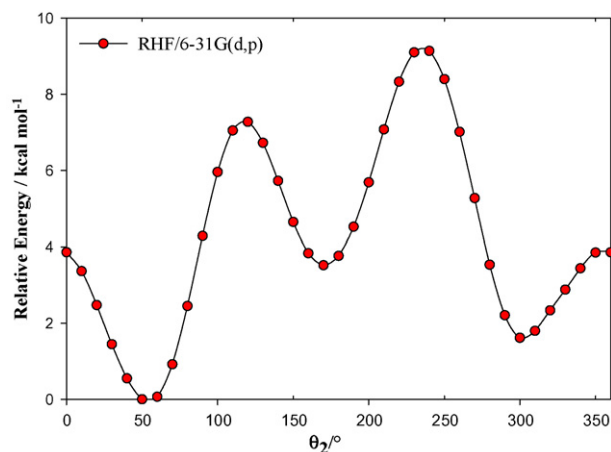


Fig. 7. Conformational energy of *N*-protonated MDMA as a function of rotation angle θ_2 in *vacuo* at the RHF/6-31G(d,p) level.

Figure, the B3LYP/6-31G(d,p) scan shows that there are three minima for MDMA, namely S_1 -like ($\theta_1 = 70^\circ$; $\theta_2 = -70^\circ$); S_2 -like ($\theta_1 = 110^\circ$; $\theta_2 = 70^\circ$); and A-like ($\theta_1 = 70^\circ$; $\theta_2 = -180^\circ$), with the latter being the lowest energy conformer. It was clear from the scan that the conformers with values of $\theta_1 = 0^\circ$; $\theta_2 = 120^\circ$ and $\theta_1 = 180^\circ$; $\theta_2 = 120^\circ$ are maxima. These results strengthen our finding that θ_1 is in fact $\sim 70^\circ$.

The PES Scan in Fig. 4 shows that there is a second minimum ~ 0.2 kcal mol $^{-1}$ higher in energy at $\theta_1 = 270^\circ$, differing from the former one as a result of the chirality of the molecule. Nevertheless, this value is well within kT at room temperature (~ 0.6 kcal mol $^{-1}$). This conformer is shown in the 3D PES Scan Fig. 6, but again the three most stable conformers are almost symmetrical to the other three, so this point is not discussed further.

3.2.5. Rotational barriers of protonated MDMA in vacuum and in polar media

The potential energy profile at the HF/6-31G(d,p) level of the conjugate acid of MDMA, neglecting medium effects and

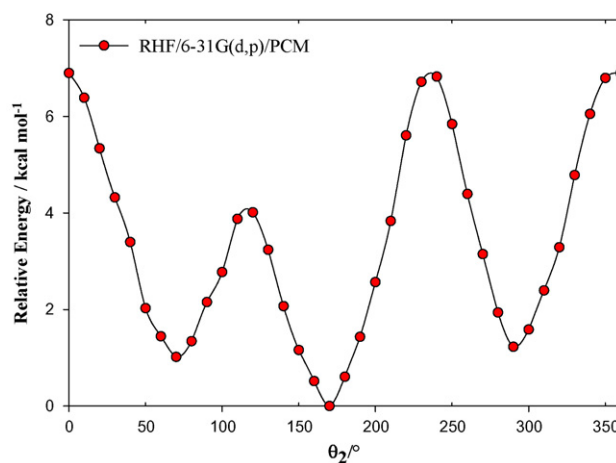


Fig. 8. Conformational energy of *N*-protonated MDMA with Cl^- as counterion as a function of rotation angle θ_2 (θ_1 optimized at 70°) at the RHF/6-31G(d,p)/PCM level ($\epsilon = 78.3$).

any influence of the counterion, is shown in Fig. 7. Large differences with respect to the neutral molecule are observed. The conformational energies found by rotation around θ_2 (with a fixed θ_1 value of 70° , PES scan results not shown) suggest that both “folded” conformations are more stable than the “extended” rotamer A, and that S_1 corresponds to the favored overall minimum. These results are in complete disagreement with the conformer distribution obtained from the experimental data (see Table 1). It may be mentioned that a similar apparent failure of the semiempirical AM1 methodology to account for the relative abundance of the conformers of *N*-protonated dopamine in polar media has been reported [27].

To account for the influence of the counterion on the internal rotation of the system, the chloride ion was then incorporated in our calculations *in vacuo*, but the results remained unchanged. Thus, we decided to include solvent polarity effects to study the conformer distribution, assuming $\epsilon = 78.3$. PCM calculations at the HF/6-31G(d,p) level carried out for different values of the N–H(Cl) and (N)H–Cl distances (*i.e.* N–H(Cl) = 1.15 Å and (N)H–Cl = 2.0 Å were the best initial values) for the most important conformers ($\theta_1 \approx 70^\circ$ and $\theta_2 \approx -180^\circ$) gave the relative internal rotation energy of θ_2 at a fixed $\theta_1 = 70^\circ$ as shown in Fig. 8. These results, showing that the *anti* rotamer A is the most stable one, are now in agreement with the experimental data. The Mulliken net atomic population was recorded to account for the relative ionic character of the system in the polar solvent, all three rotamers showing a charge of -0.98 a.u. on the chlorine atom, which means that a tight MDMAH⁺Cl[−] ion pair is being described.

The trifluoroacetic acid (TFA)–MDMA system was studied *in vacuo* to model the dilute solution in CDCl₃ used in the NMR experiments. The results revealed the same behaviour found for MDMA–HCl, *i.e.*, an absolute minimum near $\theta_1 \approx 60^\circ$, contrary to that indicated by experiment. The optimal N–H(TFA) distance was found to be 1.94 Å, and the H–O(TFA) distance was 0.99 Å obtained by AM1 [28], while the corresponding values calculated by PM3 [29] were 1.78 Å and 0.98 Å, respectively, indicating that the nitrogen atom is not protonated, and that this system is therefore not an ion pair.

A thorough study of the conformational space of phenethylamine and its conjugate acid *in vacuo*, using SCF *ab initio* and semiempirical methodologies, indicated that the neighboring preferred rotamers – regardless of the method used – differ in energy by no more than 4 kcal mol^{−1} [30]. Furthermore, the lowest energy path connecting these minima crosses saddle points which, in the worst cases (given by CNDO and INDO calculations), lie about 7 kcal mol^{−1} above a local minimum. In this work EHT (Extended Hückel Theory) calculations indicated energy barriers barely exceeding 4 kcal mol^{−1}. The unsubstituted phenethylamine and its protonated form, therefore, appear to be very mobile molecules in which the amine side chain oscillates around a plane perpendicular to the ring plane and where there is some preference for the rotamer with a *trans* relationship between the aromatic ring and the amine nitrogen atom. The less hindered *gauche* conformation, however, contributes significantly to the equilibrium mixture although it is able to interconvert quite freely with the dominant

trans form. This situation seems to be fairly general, regardless of the presence of substituents on the benzene ring or replacement of this moiety by an aromatic heterocycle, and even hydroxyl groups on the side chain carbon atom C8.

The methods used in this paper do not describe dispersion, and it is now known that this can lead to distorted energy profiles for flexible molecules containing an aromatic ring [31]. Although we do not have any indication on the relative importance of dispersion for the MDMA molecule, it seems unlikely that this effect is of similar magnitude to that observed for the “book” conformation of glycyltyrosine, as in our case the size of the substituent that can approach the aromatic ring is much less.

3.3. Crystallographic results

MDMA hydrochloride is known to crystallize in several hydrated forms, depending on how it is prepared, but none of these seem to have been fully characterized [1]. The melting characteristics of the tabular crystals obtained from MDMA hydrochloride mother liquors indicated that they might correspond to a hydrate. This was confirmed by the crystal structure of this material (M2, Table 2, Fig. 2) which, compared with the published data for anhydrous MDMA hydrochloride (M1) [11], showed that they differ in the following aspects: (a) the cell volume of M2 is larger than that of M1, in order to accommodate the water molecule; (b) they crystallize in

Table 2
Crystal data for MDMA hydrochloride monohydrate

Chemical formula	C ₁₁ H ₁₆ NO ₂ ·Cl·H ₂ O
Formula weight	247.71
Temperature (K)	120(2)
Wavelength (Å)	0.71073
Crystal system	Monoclinic
Space group	P2 ₁ /n
Unit cell dimensions (Å)	$a = 7.2437(2)$, $b = 20.8029(4)$ $c = 9.1747(2)$, $\beta = 108.225(1)$
Volume	1313.18(5)
Z	4
D_{calc} (Mg/m ³)	1.253
Absorption coefficient (mm ^{−1})	0.284
$F(0\ 0\ 0)$	528
Crystal habit	Plate
Colour	Colourless
Crystal size (mm)	0.15, 0.11, 0.09
θ -range for data collection	$\theta_{\text{min}} = 3.12$ $\theta_{\text{max}} = 25.00$
Index range	$h = 0 \rightarrow 8$, $k = 0 \rightarrow 24$, $l = -10 \rightarrow +10$
Reflections collected	4294 reflections; 2293 independent; $I > 2\sigma(I)$ 1932
Completeness to $\theta = 25^\circ$	99.2%
Refinement method	Full-matrix least squares
Data/parameters	2293/227 (including H's)
R_{sigma}	0.0259
R_{int}	0.0162
Goodness of fit on F^2	
Final R indices [$I > 2\sigma(I)$]	$R_1 = 0.0394$, $wR_2 = 0.1097$
R indices all data	$R_1 = 0.0457$, $wR_2 = 0.1168$
Largest difference peak and hole (eÅ ^{−3})	$\Delta\rho_{\text{min}} = -0.237$ $\Delta\rho_{\text{max}} = 0.186$

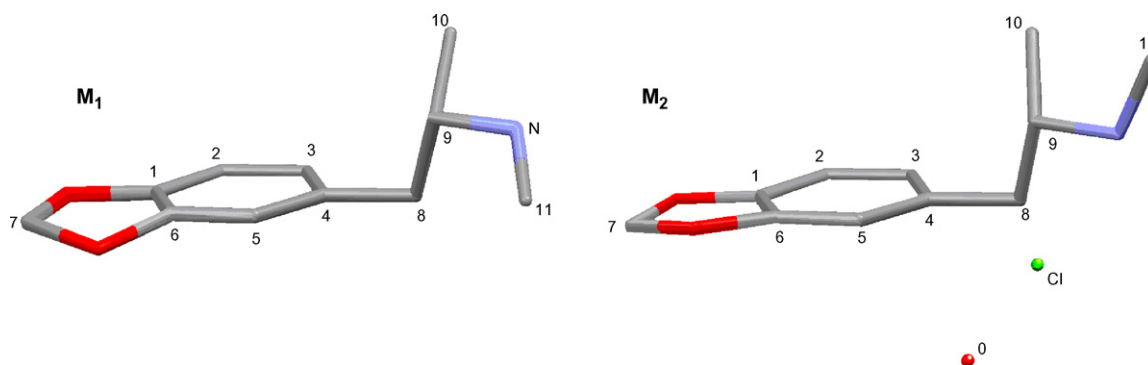


Fig. 9. Comparison of the structures of M1 and M2.

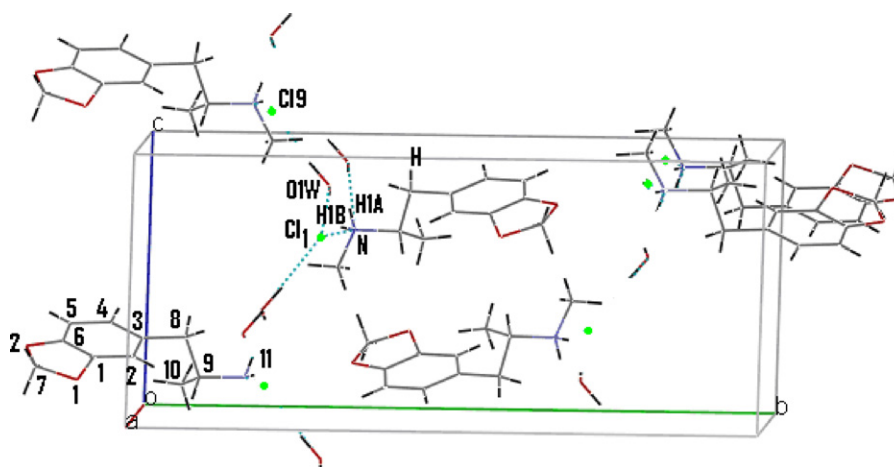


Fig. 10. Representation of the hydrogen bonding network of M2.

different crystal systems and space groups: orthorhombic $Pca2_1$ and monoclinic $P2_1/n$, for M1 and M2 respectively; (c) the conformations of M1 and M2, shown compared in Fig. 9, are essentially defined by the torsion angles around C4–C8, C8–C9, C9–N, the main difference occurring around the C9–N bond, with the *N*-methyl group *trans* to the α -methyl in M1 and *gauche* in M2 (see Table 3); (d) according to Morimoto et al. [11] in the crystal packing of the anhydrous polymorph the molecules are held together by two H-bonds involving the protonated secondary amine N and Cl11. In their structure, the distances from the chloride ion to the N atom of adjacent MDMA molecules are 3.137(2) Å and 3.089 Å. In M2, however, the molecules are held together via four H-bonds. One of these links Cl11 to N, two link Cl11 to water and one links N to water, as shown in Fig. 10 and Table 4. The M2 crystal structure is in good agreement with the *trans* rotamer obtained using *ab initio* calculations.

Table 3
Torsion angles of MDMA-HCl

Dihedral angle	Anhydrous (°)	Hydrate (°)
C11–N1–C9–C10	−170.0(2)	55.5(2)
C11–N1–C9–C8	65.9(3)	179.9(2)
C4–C8–C9–N1	172.5(2)	163.5(1)
C5–C4–C8–C9	−70.1(3)	−80.9(1)

3.4. Biological relevance

Mescaline-like activity has been reported in animals for conformationally restricted hallucinogenic phenethylamine analogues with a *trans*- (but not *cis*-) 2-arylcyclopropylamine structure [22,32]. These results are consistent with the hypothesis that phenylalkylamine hallucinogens interact with their receptors in an extended conformation. On the other hand, the more rigid 2-aminoindan and 2-aminotetralin analogs of the

Table 4
Possible hydrogen bonds of MDMA hydrochloride monohydrate (all distances are in Å and angles in °)

Donor–H	Donor–Acceptor	H–Acceptor	DonorH–Acceptor
O1W–H1W 0.951(1)	O1W–Cl (0) 3.121(1)	H1W–Cl (0) 2.174(0)	O1W–H1W–Cl (0) 172.98(0.10)
N–H1A 0.900(1)	N–Cl (0) 3.107(2)	H1A–Cl (0) 2.248(1)	N–H1A–Cl (0) 159.53(0.10)
O1W–H2W 0.924(2)	O1W–Cl9 (1) 3.114(2)	H2W–Cl (1) 2.189(1)	O1W–H2W–Cl (1) 178.58(9)
N–H1B 0.900(2)	N–O1W (2) 2.766(2)	H1B–O1W (2) 1.873(2)	N–H1B–O1W (2) 171.25(10)

Equivalent positions: (0) x, y, z ; (1) $x - 1/2, -y - 1/2, +z - 1/2$; (2) $x + 1, +y, +z$.

hallucinogen 1-(2,5-dimethoxy-4-methylphenyl)-2-aminopropane (DOM, STP), which also mimic *trans* conformations, do not elicit hallucinogen-like effects in rat conditioned avoidance studies [33]. It seems reasonable to assume that they are unable to interact effectively with the appropriate receptor(s) due, precisely, to their rigidity, perhaps because they cannot mimic the preferred perpendicular orientation of the C8–C9 bond with regard to the benzene ring. However, these rigid molecules fully substitute for MDMA in animal experiments [32], suggesting that MDMA-like activity may be associated with *trans* conformations of the aminoethyl side chain. Interestingly, the rigid analogs with MDMA-like activity are also methylenedioxy-substituted in positions that are congruent with the substitution pattern of MDMA itself, which might be crucial for its characteristic effects.

It could be postulated that the non-hallucinogenic aminoindan and aminotetralin analogs are unable to adopt more compact structures as a prerequisite for them to reach their binding site(s), which are believed to be embedded in the seven transmembrane helix bundle of 5-HT₂ serotonin receptors [34,35]. In contrast, the MDMA-like activity of its aminoindan and aminotetralin analogs might indicate that the biological targets involved, *i.e.* monoamine transporters, are able to bind effectively to “extended” conformers, not requiring the adoption of “folded” conformations *en route* from the extracellular space.

In our view, lacking highly reliable models of G-protein-coupled receptors and monoamine transporters, the most useful approach to test this hypothesis is the experimental study of the microdynamics of drug molecules supplemented by quantum-mechanical calculations of the energy barriers associated with conformational change, modelling the presence of a polarizable medium and introducing appropriate mimics (*i.e.* carboxylate ions, hydrogen bond donors or acceptors, etc.) of receptor binding site functionalities when these are known.

In the case of entactogens like MDMA, not only is there considerable uncertainty regarding their more relevant site(s) of action, but also knowledge of the structure of some of the candidate sites (*e.g.* the serotonin transporter) is far too incomplete for molecular modelling analyses to be possible at this time. Nevertheless, our results are in agreement with the hypothesis that MDMA and pharmacologically similar substances act predominantly at different macromolecular targets from those involved in the characteristic actions of the structurally related hallucinogens.

4. Conclusions

α -Methyl substitution modifies the relative stabilities of phenethylamine conformers. Upon α -methylation, rotation around the side chain C8–C9 bond is restricted and the “extended” rotamer A becomes more dominant. This effect is accentuated in CDCl₃, which may better mimic the interior of a protein molecule, relative to D₂O [21]. Nevertheless, the contribution of less favored conformations is not negligible, suggesting that the different rotamers of these molecules are still able to interconvert quite easily. Methylation of the amine

nitrogen atom could be expected to further restrict the mobility of the side chain, as has been shown by an analysis of ¹H NMR chemical shifts for the amphetamine–methamphetamine pair [22]. However, our results indicate that the preferred “extended” (A) and the less unstable *gauche* rotamer (S₁) should be in rapid equilibrium in aqueous and in nonpolar media.

Acknowledgments

This work was supported by Proyecto INI 06/03-2 Universidad de Chile, Proyecto Conicyt Bicentenario de Insercion Academica-2004, FONDECYT grant 2000009, the Presidential Chair in Sciences (BKC), and ICM grant no. P99-031-F (Chile), and FAPESP and CNPq (Brazil). YPM and JE are grateful to CNPq for research fellowships.

References

- [1] A.T. Shulgin, A. Shulgin, PIHKAL – Phenethylamines I Have Known And Loved, Transform Press, Berkeley, CA, 1991, p. 773.
- [2] D.E.J. Nichols, Differences between the mechanism of action of MDMA, MBDB and the classic hallucinogens. Identification of a new therapeutic entactogen class, *Psychoactive Drugs* 18 (1986) 305–313.
- [3] K. von Sydow, R. Lieb, H. Pfister, M. Höfler, H.-U. Wittchen, Use, abuse and dependence of ecstasy and related drugs – a transient phenomenon? Results from a longitudinal community study, *Drug Alcohol Dep.* 66 (2002) 147–159.
- [4] J. Strate, J.E. Lee, H. Wechsler, Increased MDMA use among college students: Results of a national survey, *J. Adolesc. Health* 30 (2002) 64–72.
- [5] C. Chipana, J. Camarasa, D. Pubill, E. Escubedo, Protection against MDMA-induced dopaminergic neurotoxicity in mice by methyllycarnitine: Involvement of nicotinic receptors, *Neuropharmacology* 51 (2006) 885–895.
- [6] E.S. Vizi, B. Rozsa, A. Mayer, J.P. Kiss, T. Zelles, B. Lendvai, Further evidence for the functional role of nonsynaptic nicotinic acetylcholine receptors, *Eur. J. Pharmacol.* 500 (2004) 499–508.
- [7] S. Seidel, E.A. Singer, H. Just, H. Farhan, P. Scholze, O. Kudlacek, M. Holy, K. Koppatz, P. Krivanek, M. Freissmuth, H.H. Sitte, Amphetamines take two to tango: an oligomer-based counter-transport model of neurotransmitter transport explores the amphetamine action, *Mol. Pharmacol.* 67 (2005) 140–151.
- [8] D.V. Herin, S. Liu, T. Ullrich, K.C. Rice, K.A. Cunningham, Role of the serotonin 5-HT_{2A} receptor in the hyperlocomotive and hyperthermic effects of (+)-3,4-methylenedioxymethamphetamine, *Psychopharmacology (Berl.)* 178 (2004) 505–513.
- [9] W. Klingler, J.J.A. Heffron, K. Jurkat-Rott, G. O’Sullivan, A. Alt, F. Schlesinger, J. Bufler, F. Lehmann-Horn, 3,4-Methylenedioxymethamphetamine (ecstasy) activates skeletal muscle nicotinic acetylcholine receptors, *J. Pharmacol. Exp. Ther.* 314 (2005) 1267–1273.
- [10] R. Doblin, A clinical plan for MDMA (Ecstasy) in the treatment of posttraumatic stress disorder (PTSD): partnering with the FDA, *J. Psychoactive Drugs* 34 (2002) 185–194.
- [11] B. Morimoto, S. Lovell, B. Kahr, Ecstasy: 3, 4-methylenedioxymethamphetamine (MDMA), *Acta Cryst. Sect. C* (1998) 229–231.
- [12] Enraf Nonius, COLLECT, Nonius BV; Delft, The Netherlands, 1997–2000.
- [13] Z. Ortinowski, W. Minor, C.W. Carter Sweet Jr., *Methods in Enzymology*, vol. 276, Academic Press, New York, 1997, p. 307.
- [14] G.M. Sheldrick, SHELXS-97; Program for Crystal Structure Refinement, University of Göttingen, Germany, 1997.
- [15] L.J. Farrugia, WinGX Suite for Single Crystal Small Molecule Crystallography, *J. Appl. Cryst.* 32 (1999) 837–838.

- [16] M.J. Frisch, G.W. Trucks, H.B. Schlegel, G.E. Scuseria, M.A. Robb, J.R. Cheeseman, V.G. Zakrzewski, J. A. Montgomery Jr., R.E. Stratmann, J.C. Burant, S. Dapprich, J.M. Millam, A.D. Daniels, K.N. Kudin, M.C. Strain, O. Farkas, J. Tomasi, V. Barone, M. Cossi, R. Cammi, B. Mennucci, C. Pomelli, C. Adamo, S. Clifford, J. Ochterski, G.A. Petersson, P.Y. Ayala, Q. Cui, K. Morokuma, P. Salvador, J.J. Dannenberg, D.K. Malick, A.D. Rabuck, K. Raghavachari, J.B. Foresman, J. Cioslowski, J.V. Ortiz, A.G. Baboul, B.B. Stefanov, G. Liu, A. Liashenko, P. Piskorz, I. Komaromi, R. Gomperts, R.L. Martin, D.J. Fox, T. Keith, M.A. Al-Laham, C.Y. Peng, A. Nanayakkara, C. Gonzalez, M. Challacombe, P.M.W. Gill, B. Johnson, W. Chen, M.W. Wong, J.L. Andres, C. Gonzalez, M. Head-Gordon, E.S. Replogle, J.A. Pople, Gaussian98; Revision A.11.3, Gaussian, Inc., Pittsburgh, PA, 1998.
- [17] M. Persico, J. Tomasi, Molecular Interactions in Solution: An Overview of Methods Based on Continuous Distributions of the Solvent, *Chem. Rev.* 94 (1994) 2027–2094.
- [18] M. Karplus, Vicinal proton coupling in nuclear magnetic Resonance, *Am. Chem. Soc.* 85 (1963) 2870–2871.
- [19] K. Bailey, Analysis of NMR spectra for rotamer populations of dimethoxyamphetamines, *J. Pharm. Sci.* 60 (1971) 1232–1233.
- [20] C.A.G. Haasnoot, F.A.A.M. DeLeeuw, C. Altona, The relationship between proton-proton NMR coupling constants and substituent electronegativities—I, *Tetrahedron* 36 (1980) 2783–2792.
- [21] A. Makriyannis, J. Knittel, Conformational studies on phenethylamine hallucinogens: the role of alpha alkyl substitution, in: G. Barnett, M. Trsic, R.E. Willette (Eds.), NIDA Research Monograph Series 22, U.S. Government Printing Office, Washington, D.C., 1978, pp. 464–478.
- [22] G.A. Neville, R. Deslauriers, B.J. Blackburn, I.C.P. Smith, Conformational studies of amphetamine and medicinally important derivatives by nuclear magnetic resonance spectroscopy, *J. Med. Chem.* 14 (1971) 717–721.
- [23] R.J. Abraham, G. Gatti, Rotational isomerism. Part VI. Effect of substituents on vicinal coupling constants in XCH₂. CH₂Y fragments, *J. Chem. Soc. (B)* (1969) 961–968.
- [24] M.L. Huggins, Bond energies and polarities, *J. Am. Chem. Soc.* 75 (1953) 4123–4126.
- [25] P.R. Wells, Group electronegatives, *Progr. Phys. Org. Chem.* 6 (1968) 111–146.
- [26] A. Makriyannis, J. Knittel, Conformational analysis of amphetamines in solution based on unambiguous assignment NMR Spectra, *Tetrahedron Lett.* 22 (1981) 4631–4634.
- [27] J.J. Urban, C.J. Cramer, G.R. Famini, A Computational Study of Solvent Effects on the Conformation of Dopamine, *J. Am. Chem. Soc.* 114 (1992) 8226–8231.
- [28] M.J.S. Dewar, E.G. Zoebisch, E.F. Healy, J.J.P. Stewart, AM1: A new general purpose quantum mechanical model, *J. Am. Chem. Soc.* 107 (1985) 3902–3909.
- [29] J.J.P. Stewart, Optimization of parameters for semiempirical methods I, *Method J. Comput. Chem.* 10 (1989) 209–220.
- [30] M. Martin, R. Carbó, C. Petrongolo, J. Tomasi, Structure-activity relationships of phenethylamine. A comparison of quantum mechanical SCF “ab initio” and semiempirical calculations, *J. Am. Chem. Soc.* 97 (1975) 1338–1347.
- [31] T. van Mourik, P.G. Karamertzanis, S.L. Price, Molecular Conformations, Relative stabilities can be as demanding of the electronic structure method as intermolecular calculations, *J. Chem. Phys. A* 110 (2006) 8–12.
- [32] P.D. Cooper, G.C. Walters, Stereochemical requirements of the mescaline receptor, *Nature* 238 (1972) 96–98.
- [33] F.A.B. Aldous, B.C. Barras, K. Brewster, D.A. Buxton, D.M. Green, R.M. Pinder, P. Rich, M. Skeels, K.J. Tutt, Structure-Activity relationships in psychotomimetic phenylalkylamines, *J. Med. Chem.* 17 (1974) 1100–1111.
- [34] D.E. Nichols, C.F. Barfknecht, J.P. Long, R.T. Standridge, H.G. Howell, R.A. Partyka, D.C. Dyer, Rigid analogs of 2,5-dimethoxy-4-methylphenyl- isopropylamine (DOM, STP), *J. Med. Chem.* 17 (1974) 161–166.
- [35] R.A. Glennon, R. Raghupathi, P. Bartyzel, M. Titeler, S. Leonhardt, Binding of phenylalkylamine derivatives at 5-HT_{1C} and 5-HT₂ serotonin receptors: evidence for a lack of selectivity, *J. Med. Chem.* 35 (1992) 734–740.